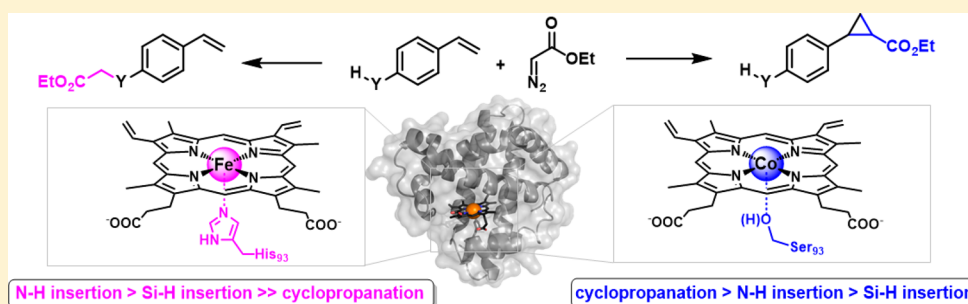


Chemoselective Cyclopropanation over Carbene Y–H Insertion Catalyzed by an Engineered Carbene Transferase

Eric J. Moore,[†] Viktoria Steck,[†] Priyanka Bajaj, and Rudi Fasan*[†]

Department of Chemistry, University of Rochester, Rochester, New York 14627, United States

S Supporting Information



ABSTRACT: Hemoproteins have recently emerged as promising biocatalysts for promoting a variety of carbene transfer reactions including cyclopropanation and Y–H insertion (Y = N, S, Si, B). For these and synthetic carbene transfer catalysts alike, achieving high chemoselectivity toward cyclopropanation in olefin substrates bearing unprotected Y–H groups has proven remarkably challenging due to competition from the more facile carbene Y–H insertion reaction. In this report, we describe the development of a novel artificial metalloenzyme based on an engineered myoglobin incorporating a serine-ligated Co-porphyrin cofactor that is capable of offering high selectivity toward olefin cyclopropanation over N–H and Si–H insertion. Intramolecular competition experiments revealed a distinct and dramatically altered chemoselectivity of the Mb-(H64V,V68A,H93S)[Co(ppIX)] variant in carbene transfer reactions compared to myoglobin-based variants containing the native histidine-ligated heme cofactor or other metal/proximal ligand substitutions. These studies highlight the functional plasticity of myoglobin as a “carbene transferase” and illustrate how modulation of the cofactor environment within this metalloprotein scaffold represents a valuable strategy for accessing carbene transfer reactivity not exhibited by naturally occurring hemoproteins or transition metal catalysts.

INTRODUCTION

The transition-metal catalyzed insertion of carbenoids into C=C, C–H, and Y–H bonds (Y = N, S, O, Si, B) represents an important class of transformations for the construction of new carbon-carbon and carbon-heteroatom bonds.¹ A plethora of organometallic catalysts, including Rh-, Ir-, Ru-, Cu-, Co-, and Fe-based complexes, have been reported to promote these transformations.¹ More recently, our group and others have demonstrated the ability of engineered hemoproteins derived from myoglobin² and cytochrome P450s,³ respectively, to provide viable biocatalysts for mediating olefin cyclopropanations as well as other types of carbene-mediated transformations, including N–H insertion,⁴ S–H insertion,⁵ and Si–H insertion.⁶ Artificial “carbene transferases” based on these^{2,7} or other protein scaffolds⁸ have also been reported.

Among carbene-mediated transformations, olefin cyclopropanations are particularly attractive owing to the relevance of cyclopropane rings as structural motifs in medicinal chemistry and drug discovery.⁹ Despite major progress made in transition metal-catalyzed carbene transfer chemistry,¹ the development of catalytic systems capable of favoring olefin cyclopropanation over carbene Y–H insertion reactions has

remained an unmet challenge. Indeed, studies involving different types of organometallic catalysts invariably showed that the more facile Y–H carbene insertion outcompetes olefin cyclopropanation in both inter- and intramolecular settings.¹⁰ A similar reactivity trend is exhibited by hemoprotein-based carbene transfer catalysts as documented by our own studies (*vide infra*) and reports from other groups.^{4a,6} Indeed, Arnold and co-workers reported the exclusive occurrence of N–H insertion in the P450-catalyzed transformation of *p*-aminostyrene with ethyl α -diazoacetate^{4a} and exclusive formation of the Si–H insertion product in the cytochrome *c*-catalyzed transformation of a silane group-containing styrene derivative with ethyl α -diazoacetate.⁶ In this context, the development of carbene transfer catalysts capable of favoring cyclopropanation in substrates bearing unprotected Y–H groups is highly desirable as these systems would not only complement the chemoselectivity of (bio)catalysts currently

Special Issue: Organic and Biocompatible Transformations in Aqueous Media

Received: April 20, 2018

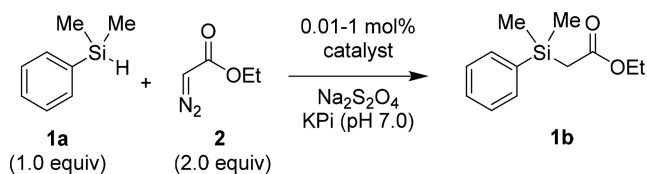
Published: June 15, 2018

available for these reactions, but also disclose new opportunities toward the selective cyclopropanation of densely functionalized olefin substrates. Herein, we report the development and characterization of a myoglobin-based biocatalyst that is able to display high chemoselectivity toward olefin cyclopropanation over N–H and Si–H insertion, a unique reactivity acquired through substitution of the native histidine-ligated heme cofactor with a non-native serine-ligated Co-porphyrin.

RESULTS AND DISCUSSION

At the incipit of these studies, we selected the Mb(H64V,V68A) variant as the starting point for catalyst development in reason of its high catalytic activity (>10,000 turnovers (TON)) and stereoselectivity (95–99% de and ee) in the cyclopropanation of vinylarene substrates in the presence of ethyl α -diazoacetate (EDA) as the carbene donor.^{2a} This variant also exhibits high activity toward the functionalization of arylamines^{4b} and mercaptan substrates⁵ with diazoester reagents via carbene N–H and S–H insertion, respectively. Carbene insertion into the Si–H bonds of silanes is a facile transformation for carbene transfer catalysts.¹¹ To assess the Si–H insertion activity of Mb(H64V,V68A), we examined the transformation of dimethylphenyl silane (**1a**) in the presence of EDA (**2**) to give the functionalized product **1b** (Table 1). As expected, this reaction proceeded efficiently,

Table 1. Myoglobin-Catalyzed Carbene Si–H Insertion with Dimethylphenyl Silane **1a and EDA **2**^a**



entry	catalyst	cat. loading	% yield ^b	TON
1	hemin	1 mol %	15	15
2	Mb	0.2 mol %	35	175
3	Mb(H64V,V68A)	0.2 mol %	66	330
4	Mb(H64V,V68A)	0.01 mol %	15	1545

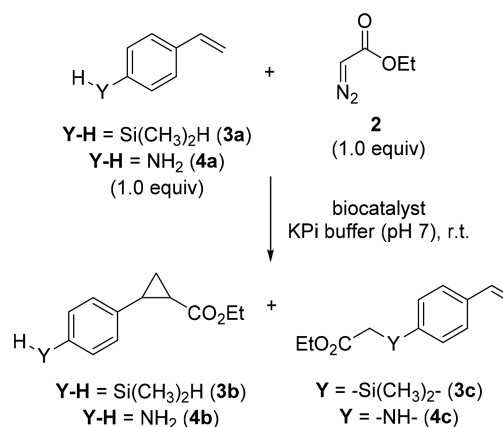
^aReaction conditions: 10 mM dimethylphenyl silane, 20 mM EDA, 10 mM Na₂S₂O₄, 1–100 μ M catalyst in 50 mM phosphate buffer (pH 7.0). ^bBased on GC conversion using calibration curves with isolated **1b**.

resulting in the clean formation of the Si–H insertion product in 66% yield in the presence of 0.2 mol % catalyst (330 TON; Table 1, entry 3). By comparison, negligible Si–H insertion activity was observed for free hemin (15 TON; Table 1, entry 1), whereas wild-type sperm whale myoglobin (Mb) displayed a 2-fold lower activity compared to the Mb(H64V,V68A) variant (175 TON; Table 1, entry 2). Under catalyst-limited conditions, Mb(H64V,V68A) was found to support over 1,500 turnovers in this reaction (Table 1, entry 4). This catalytic activity compares favorably with that recently reported for the same silane substrate and ethyl α -diazoacetate by an engineered cytochrome *c* variant optimized by directed evolution for this reaction (2,520 TON)⁶ or that of other metalloprotein/protein complexes investigated in the context of related Si–H insertion reactions.¹² Altogether, these results demonstrated that Si–H insertion reactions are readily catalyzed by the Mb-based “carbene transferase” as expected

based on its previously observed reactivity toward other electron-rich Y–H substrates.^{4b,5}

On the basis of these results, we were interested in assessing the chemoselectivity of Mb(H64V,V68A) in the cyclopropanation of 4-(dimethylsilyl)styrene (**3a**) in which the silane group (Si–H) can compete for carbene insertion with the olefinic group (Table 2). This reaction led to minimal

Table 2. Chemoselectivity of Myoglobin and Other Hemoproteins in the Reaction with 4-(Dimethylsilyl)styrene (3a**) or *para*-Amino-styrene (**4a**) and EDA^a**



entry	catalyst	% yield (3b + 3c) ^b	3b : 3c ratio	% yield (4b + 4c) ^b	4b : 4c ratio
1	Mb	6	3:97	65	1:99
2	Mb(H64V,V68A)	13	4:96	85	0:100
3	HRP	1	11:89	96	0:100
4	catalase	1	9:91	6	2:98
5	P450 _{BM3}	<0.5	5:95	24	1:99
6	FL#62	4	5:95	25	1:99
7	cytochrome <i>c</i>	10	5:95	57	1:99

^aReaction conditions: 10 mM **3a** or **4a**, 10 mM EDA, 10 mM Na₂S₂O₄, 20 μ M catalyst in 50 mM phosphate buffer (pH 7.0).

^bBased on GC conversion using calibration curves with isolated **3b**, **3c**, **4b**, and **4c**.

formation (4%) of the desired cyclopropane product **3b** with the Si–H insertion adduct **3c** representing the largely predominant product (96%; Table 2, entry 2). Albeit with lower efficiency (1–10% vs 13% conv.), a similar reactivity profile was observed for a variety of other hemoproteins, including horseradish peroxidase (HRP), catalase, cytochrome P450_{BM3} and its engineered variant FL#62,¹³ and cytochrome *c* (Table 2, entries 3–7) with which the cyclopropanation product **3b** is formed only in minor amounts (<5–11%) compared to the Si–H insertion product. The results with wild-type equine heart cytochrome *c* are consistent with those recently reported in a related reaction with cytochrome *c* from *Rhodothermus marinus*.⁶

To examine the relative reactivity toward olefin cyclopropanation vs N–H insertion, similar experiments were conducted in the presence of *para*-amino-styrene (**4a**) and EDA as the carbene donor reagent. Interestingly, in addition to Mb(H64V,V68A), horseradish peroxidase and cytochrome *c* were found to be particularly active in the transformation of this substrate, leading to the N–H insertion product in 96 and 57% yields, respectively (Table 2, entries 3 and 7). For these and all the other hemoproteins, however, the desired

cyclopropanation product **3b** was either not formed (HRP) or produced only in negligible amounts (<1–2%). Along with observations previously made with synthetic catalysts,^{10a–c} these results corroborated the notion that preferential formation of the cyclopropanation product in substrates containing an unprotected Si–H or N–H group is not attainable using currently available carbene transfer catalysts and biocatalysts.

The carbene transfer activity of Mb hinges upon the formation of a carbene-heme intermediate at the level of the active site (i.e., distal heme pocket),^{2a} whose reactivity is influenced by the nature of the porphyrin ligand and axial residue.¹⁴ Previously, we established that modification of the metalloporphyrin cofactor environment within this scaffold, i.e., through substitution of the metal,^{2c} porphyrin ligand,^{7a} or metal-ligating proximal residue,¹⁴ can modulate the carbene transfer reactivity of this metalloprotein. On the basis of these findings, we hypothesized that this approach could furnish a means to tune the chemoselectivity of myoglobin-based cyclopropanation catalysts and thus access Mb variants capable of favoring olefin cyclopropanation over the inherently more facile carbene Y–H insertions in functionalized substrates where both reactions are possible (e.g., **3a** and **4a**).

Toward this goal, we prepared a library of Mb(H64V,V68A)-derived variants in which the native heme is substituted with Co(ppIX), Mn(ppIX), and Rh(mpIX). In addition, the native metal-coordinating His residue (His93) was varied to include alternative nucleophilic residues (i.e., Cys, Ser, Tyr) as well as non-Lewis basic amino acids (i.e., Ala and Phe). On the basis of the available crystal structure of Mb,¹⁵ the His93Ala and His93Phe variants were expected to alter steric access at the proximal side of the metalloporphyrin cofactor for either enabling or disfavoring, respectively, axial coordination of the metal by a water molecule. Conveniently, these artificial metalloenzymes could be produced directly in *E. coli* cells arrayed in 96-well plates by exploiting our recently introduced protocol for the recombinant expression of cofactor-substituted myoglobins.^{2c,16}

The catalytic activity and selectivity toward cyclopropanation vs Si–H insertion of the cofactor-modified Mb variants was then assessed in whole-cell reactions^{2b} containing 4-(dimethylsilyl)styrene **3a** and EDA. The results from these experiments are graphically summarized in Figure 1a, and the most representative data are provided in Table 3. Interestingly, these analyses revealed a significant impact of both the metal and proximal residues on the catalytic activity and chemoselectivity of the reaction. For example, in the presence of the native heme cofactor (Fe(ppIX)), only the His93Ser variant exhibited comparable activity to the parent protein Mb(H64V,V68A) (Table 3, entries 1 and 2). In contrast, the most active catalysts among the Mn-containing Mb variants feature a non-nucleophilic residue (i.e., Ala or Phe) in place of the proximal histidine residue (Table 3, entries 3–5). More importantly, heme replacement with the non-native cofactor Co-protoporphyrin IX (Co(ppIX)) induced a dramatic shift in the chemoselectivity of the Mb catalyst to favor the formation of the cyclopropanation product, leading to **3b**:**3c** ratios ranging from 40:60 to 74:26 (Figure 1a). This reactivity is in stark contrast with that of the Fe-, Mn-, and Rh-containing variants, which greatly favor the formation of the Si–H insertion product (**3b**:**3c** ratios from 4:96 to 11:89; Figure 1a).

Among the Co-substituted variants, Mb(H64V,V68A,H93S)[Co(ppIX)] displayed the most optimal

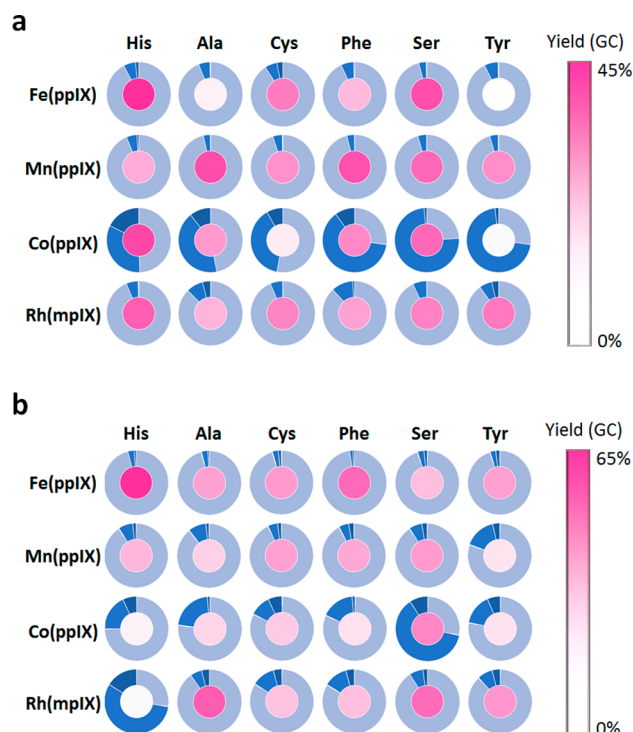
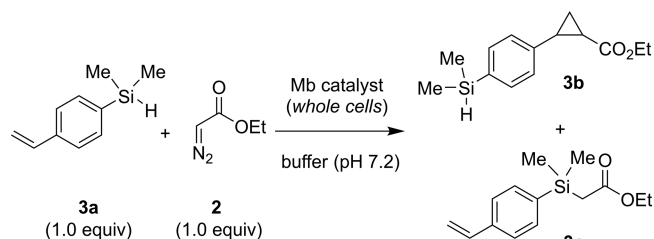


Figure 1. Screening data for the cofactor/proximal ligand-substituted Mb(H64V,V68A) variants in the reactions with (a) 4-(dimethylsilyl)styrene **3a** or (b) 4-amino-styrene **4a**, and EDA. The pie charts indicate the product distribution (light blue for Si–H and N–H insertion products **3c** and **4c**, respectively; blue for cyclopropanation product **3b** and **4b**, respectively; dark blue for multiple insertion byproduct(s)). The activity (% GC yield) is represented as filling color.

Table 3. Catalytic Activity and Selectivity of Selected Mb(H64V,V68A) Variants in the Reaction with 4-(Dimethylsilyl)styrene (**3a**) and EDA^a



entry	protein	cofactor	% yield ^b	% 3b ^c	% 3c ^c
1	Mb(H64V,V68A)	Fe(ppIX)	41	6	92
2	Mb(H64V,V68A,H93S)	Fe(ppIX)	36	4	96
3	Mb(H64V,V68A)	Mn(ppIX)	18	5	94
4	Mb(H64V,V68A,H93A)	Mn(ppIX)	36	3	96
5	Mb(H64V,V68A,H93F)	Mn(ppIX)	35	4	96
6	Mb(H64V,V68A)	Co(ppIX)	37	33	49
7	Mb(H64V,V68A,H93S)	Co(ppIX)	44	74	24
8	Mb(H64V,V68A,H93F)	Co(ppIX)	25	63	10
9	Mb(H64V,V68A)	Rh(mpIX)	33	6	94

^aReaction conditions: 10 mM **3a**, 10 mM EDA, *E. coli* whole cells expressing Mb variant (OD₆₀₀ = 40) in 50 mM phosphate buffer (pH 7.2). ^bBased on GC conversion using calibration curves with isolated **3b** and **3c**. ^cThe remainder to 100% corresponds to double insertion product(s).

combination of high chemoselectivity for cyclopropanation over Si–H insertion (74% selectivity) and good catalytic activity (Table 3, entry 7). Attempts to further optimize the Mb(H64V,V68A,H93S)[Co(ppIX)]-catalyzed reaction by varying the substrate loading and/or 3a:EDA ratio did not result in significant improvements in the yield of 3b, indicating that the reaction conditions applied during the catalyst screening were already optimal for this transformation.

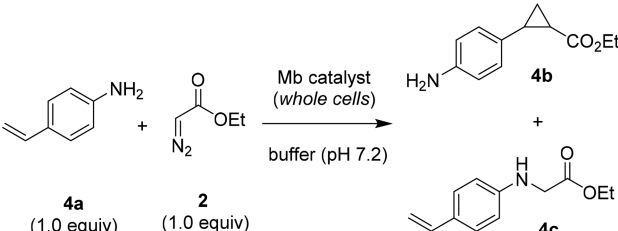
From the systematic set of structure–activity data collected in these experiments, it became apparent that, whereas the cobalt metal center is critical for inducing the desired selectivity toward cyclopropanation (6% → 33%; Table 3, entry 6 vs 1), axial coordination by the serine residue is beneficial toward enhancing this reactivity (33% → 74%; Table 3, entry 7 vs 6). Control experiments using free Co(ppIX) as the catalyst (2 mol %) under identical reaction conditions (10 mM 3a, 10 mM EDA, 10 mM Na₂S₂O₄ in phosphate buffer, pH 7.2) resulted in negligible formation of product (<1% yield), most of which consisted of the Si–H insertion product (80%). These results further evidenced the critical role of the protein matrix in modulating the reactivity and selectivity of the Co-protoporphyrin IX cofactor.

Encouraged by these results, the panel of Mb(H64V,V68A)-based variants was screened against 4-amino-styrene (4a) in which carbene insertion into the N–H bond of the amino group was found to greatly outcompete cyclopropanation of the C=C bond in the reactions catalyzed by Mb(H64V,V68A) and other carbene transfer (bio)catalysts (Table 2). As shown by the data summarized in Figure 1b, also in this case substitution of the metal and axial ligand was found to significantly alter the efficiency and/or chemoselectivity of the reaction. Specifically, all the Fe-containing variants maintain high preference for the N–H insertion reaction (95–96%) over the cyclopropanation reaction regardless of the nature of the proximal residue. Most of these variants also display significantly reduced activity compared to Mb(H64V,V68A) with the only exception being the H93F variant, whose catalytic activity is only moderately affected (47 vs 63% yield; Table 4, entry 2 vs 1).

In comparison, metal substitution appeared to have a more profound impact on the chemoselectivity of the metalloprotein catalyst. Across the board, the Co-substituted variants displayed a more pronounced propensity to promote the formation of the cyclopropanation product 4b (10–62% selectivity; Figure 1b) when compared to the Mn-containing variants and most of the Rh-containing variants (5–15% selectivity).

As observed for the Si–H insertion vs cyclopropanation reaction with 3a, the Mb variant combining the Co(ppIX) and His93Ser substitution emerged as the most efficient and chemoselective catalyst for promoting the cyclopropanation of 4a to give the desired product 4b (62% selectivity; Table 4, entry 7). Again, coordination of the cobalt center by the serine residue appears to be critical for enhancing this chemoselectivity feature, as evidenced by the 3- to 6-fold higher selectivity of this variant toward favoring cyclopropanation over N–H insertion when compared to both the histidine-ligated and the structurally similar cysteine-ligated counterparts (Table 4, entry 7 vs 5 and 6). The Mb(H64V,V68A,H93S)-[Co(ppIX)]-catalyzed conversion of 4a could be further optimized to yield the cyclopropanation product 4b with 72% selectivity in 45% yield (Table 3, entry 8). Control reactions with free Co(ppIX) cofactor in buffer show minimal conversion of 4a to a mixture of 4b and 4c (<1% yield).

Table 4. Catalytic Activity and Selectivity of Selected Mb(H64V,V68A) Variants in the Reaction with 4-Amino-styrene (4a) and EDA^a



entry	protein	cofactor	% yield ^b	% 4b ^c	% 4c ^c
1	Mb(H64V,V68A)	Fe(ppIX)	63	3	96
2	Mb(H64V,V68A,H93F)	Fe(ppIX)	47	2	98
3	Mb(H64V,V68A)	Mn(ppIX)	25	7	91
4	Mb(H64V,V68A,H93Y)	Mn(ppIX)	11	16	81
5	Mb(H64V,V68A)	Co(ppIX)	6	18	75
6	Mb(H64V,V68A,H93C)	Co(ppIX)	19	10	83
7	Mb(H64V,V68A,H93S)	Co(ppIX)	38	62	28
8 ^d	Mb(H64V,V68A,H93S)	Co(ppIX)	45	72	24
9	Mb(H64V,V68A)	Rh(mpIX)	4	56	28
10	Mb(H64V,V68A,H93A)	Rh(mpIX)	50	6	90

^aReaction conditions: 10 mM 4a, 10 mM EDA, *E. coli* whole cells expressing Mb variants (OD₆₀₀ = 40) in 50 mM phosphate buffer (pH 7.2). ^bBased on GC conversion using calibration curves with isolated 4b and 4c. ^cThe remainder to 100% corresponds to double insertion product(s). ^dWith 10 mM 4a, 7.5 mM EDA, and whole cells at OD₆₀₀ = 80.

Interestingly, the Rh-based variant Mb(H64V,V68A)[Rh(mpIX)] also exhibited significantly improved selectivity toward cyclopropanation vs N–H insertion compared to the parent variant Mb(H64V,V68A) (3% → 56% selectivity; Table 4, entry 9 vs 1). However, this change in chemoselectivity is accompanied by a drastic reduction in catalytic activity, making it an inferior catalyst compared to Mb(H64V,V68A,H93S)-[Co(ppIX)]. Still, it is interesting to note the distinctive effect of the proximal histidine toward inducing the observed chemoselectivity shift in the Rh-based variant compared to the other residues introduced at this position (Figure 1b) or to the His93Ala counterpart in which axial coordination of the metal is not available (Table 4, entry 10 vs 9). As for Mb(H64V,V68A,H93S)[Co(ppIX)], these results highlight the interplay of the effects resulting from metal and proximal ligand variation in tuning the reactivity and chemoselectivity of these biocatalysts.

On the basis of these results, Mb(H64V,V68A,H93S)[Co(ppIX)] was selected for further characterization. This variant could be efficiently expressed and isolated from *E. coli* as holoprotein in good yields (~8 mg/L culture). Its UV–vis spectrum shows a strong absorption band at 425 nm and two weak absorption bands at 535 and 570 nm corresponding to the Soret and Q-bands of the protein, respectively (Figure 2a). Upon addition of sodium dithionite (Na₂S₂O₄), the Soret band shifts to 405 nm, which was assigned to the reduced Co(II) form of the metalloprotein. Unlike the iron-based counterpart, only partial reduction (~40%) of Mb(H64V,V68A,H93S)-[Co(ppIX)] was observed with excess sodium dithionite even after overnight incubation (Figure 2a, red line). More efficient conversion to the reduced form of this protein was achieved instead using the stronger reductant Ti(III) citrate in

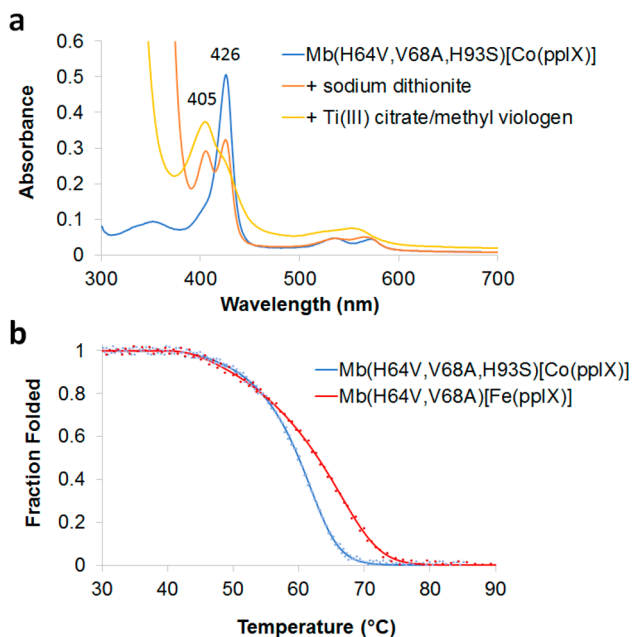


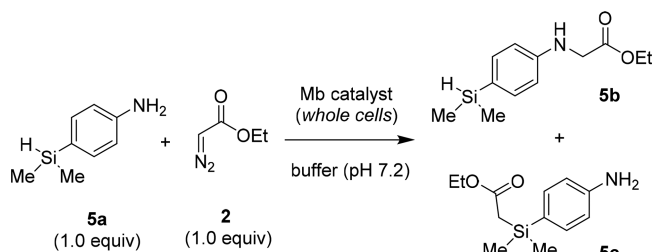
Figure 2. Characterization of Mb(H64V,V68A,H93S)-[Co(ppIX)]. (a) Overlay of the electronic absorption spectra of the protein prior to (blue) and after reduction with sodium dithionite (red) or Ti(III) citrate (orange). (b) Thermal denaturation curves for Mb(H64V,V68A) (green) and Mb(H64V,V68A,H93S)[Co(ppIX)] (red) as determined by circular dichroism (θ_{222}).

combination with the electron transfer mediator methyl viologen (Figure 2a, orange line).¹⁷

Control experiments involving reactions with **3a** or **4a** in the presence of either the oxidized or reduced form of Mb(H64V,V68A,H93S)[Co(ppIX)] revealed that the latter species is catalytically less active but more selective for cyclopropanation over Si–H (or N–H) insertion compared to the oxidized form of the protein. Moreover, both TON and the cyclopropanation vs Y–H insertion chemoselectivity obtained with the purified protein were lower than those achieved in the whole cell reactions, clearly indicating a favorable effect of the intracellular environment on the catalytic performance of this biocatalyst. This effect can be in part attributed to the efficient reduction of Mb(H64V,V68A,H93S)[Co(ppIX)] within the reducing intracellular milieu, as suggested by UV–vis spectroscopy analysis of cell lysates (Co(II):Co(III) > 9:1). Through thermal denaturation experiments using circular dichroism (CD), we further determined that the Mb(H64V,V68A,H93S)[Co(ppIX)] variant has an apparent melting temperature (T_m) of 60.0 °C ± 0.2 (Figure 2b). This T_m value is comparable to that of Mb(H64V,V68A) (66.0 °C ± 1.0),¹⁸ indicating that remodeling of the cofactor environment in this variant did not significantly affect the stability of the metalloprotein.

For gaining further insights into the chemoselectivity properties of Mb(H64V,V68A,H93S)[Co(ppIX)], this and other selected variants were tested in an intramolecular competition experiment using 4-(dimethylsilyl)aniline **5a** in which N–H insertion competes for Si–H insertion (Table 5). These studies showed that Mb(H64V,V68A,H93S)[Co(ppIX)] exhibits a strong preference toward the N–H insertion reaction over the Si–H insertion reaction (89% selectivity), a feature shared by the Fe-containing or histidine-ligated counterpart (86–92% selectivity; Table 5, entries 2 and

Table 5. Catalytic Activity and Selectivity of Selected Mb(H64V,V68A) Variants in the Reaction with 4-(Dimethylsilyl)aniline (**5a**) and EDA^a



entry	protein	cofactor	% yield ^b	% 5b ^c	% 5c ^c
1	Mb(H64V,V68A)	Fe(ppIX)	72	76	1
2	Mb(H64V,V68A,H93S)	Fe(ppIX)	25	86	3
3	Mb(H64V,V68A)	Co(ppIX)	33	92	5
4	Mb(H64V,V68A,H93S)	Co(ppIX)	23	89	5

^aReaction conditions: 10 mM **5a**, 10 mM EDA, *E. coli* whole cells expressing Mb variants ($OD_{600} = 40$) in 50 mM phosphate buffer (pH 7.2). ^bBased on GC conversion using calibration curves with isolated **5b** and **5c**. ^cThe remainder to 100% corresponds to double insertion product(s).

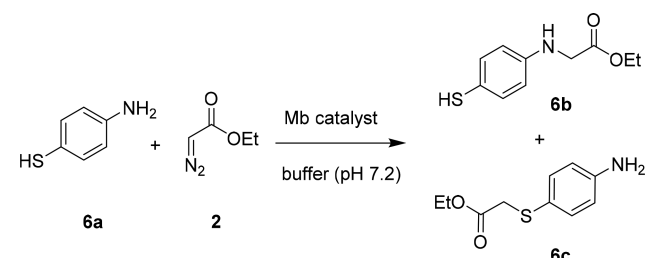
3 vs 4). In comparison, the parent variant Mb(H64V,V68A) is more active (72 vs 23% yield for Mb(H64V,V68A,H93S)[Co(ppIX)]) but less selective toward N–H insertion over the Si–H insertion and double insertion reactions (Table 4, entries 1 vs 4). From these and the previous experiments, it can be derived that the general order of reactivity for the Mb(H64V,V68A,H93S)[Co(ppIX)] variant is C=C > N–H > Si–H. This chemoselectivity is inverted compared to that of the parent Mb variant Mb(H64V,V68A) (N–H > Si–H ≫ C=C) or other hemoproteins (Table 2) and organometallic catalysts (N–H ≫ C=C).^{10a–c}

To evaluate the effect of the altered cofactor environment on the catalyst reactivity toward other types of Y–H insertions, further tests were carried out using 4-amino-thiophenol (**6a**) in which both N–H and S–H insertion reactions are possible (Table 6). Interestingly, these experiments showed that, whereas Mb(H64V,V68A) favors the N–H insertion reaction (~4:1 ratio for **6b**:**6c**; Table 6, entries 1 and 2), the Mb(H64V,V68A,H93S)[Co(ppIX)] variant features inverted chemoselectivity favoring the S–H insertion process (**6b**:**6c** ratio from 1:2 to 1:4; Table 6, entries 3 and 4). In addition, Mb(H64V,V68A,H93S)[Co(ppIX)] shows higher selectivity against the formation of the double insertion byproduct (0 vs 9–15%).

Neither Mb(H64V,V68A) nor Mb(H64V,V68A,H93S)[Co(ppIX)] were found to catalyze O–H insertion reactions as determined in experiments with phenol and EDA (no formation of ethyl 2-phenoxyacetate) and the lack of reactivity with water in the presence of EDA alone (no formation of ethyl 2-hydroxyacetate). This is unlike Rh- and other transition metal-based catalysts, which readily react with alcohols or water to give carbene O–H insertion products.^{1a,10e,19}

Having identified a biocatalyst with high chemoselectivity for cyclopropanation over N–H/Si–H insertion, we were interested in examining the impact of the modified cofactor environment on the substrate scope, catalytic activity, and selectivity of this biocatalyst in olefin cyclopropanation, as compared to the parent catalyst Mb(H64V,V68A). For this purpose, we tested a panel of representative vinylarene

Table 6. Catalytic Activity and Selectivity of Mb(H64V,V68A) and Mb(H64V,V68A,H93S)[Co(ppIX)] in the Reaction with 4-Amino-thiophenol (6a) and EDA^a

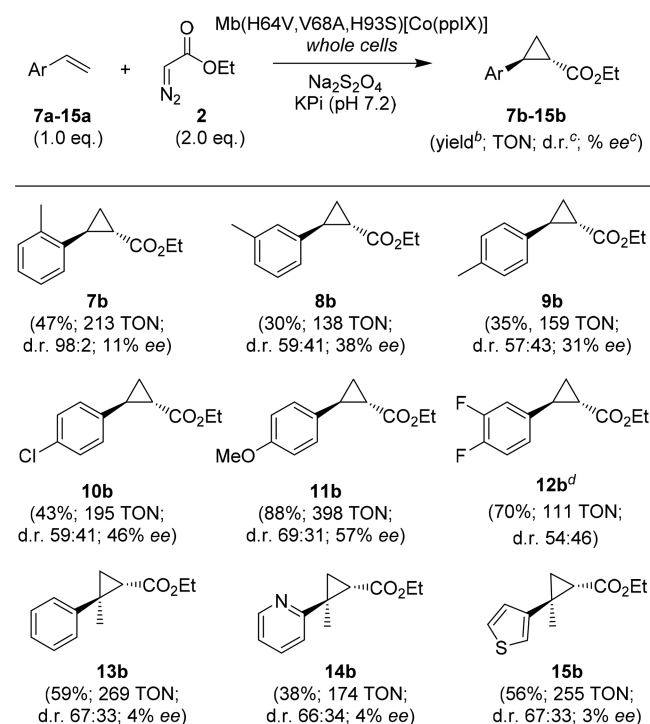


entry	protein	equiv, EDA	% yield ^b	% 6b	% 6c	% other ^c
1	Mb(H64V,V68A)	1	43	73	18	9
2	Mb(H64V,V68A)	2	76	70	15	15
3	Mb(H64V,V68A,H93S) [Co(ppIX)]	1	27	20	80	0
4	Mb(H64V,V68A,H93S) [Co(ppIX)]	2	55	35	65	0

^aReaction conditions: 3 mM 6a, 3 or 6 mM EDA, 10 mM Na₂S₂O₄, 10 mM TCEP, 20 μM purified Mb variant in 50 mM phosphate buffer (pH 7.2). ^bBased on HPLC conversion using calibration curves with isolated 6b and 6c. ^cDouble insertion product(s).

substrates (7a–15a) previously characterized in the context of Mb(H64V,V68A)-catalyzed cyclopropanation with EDA.^{2a,b} As summarized in Scheme 1, all of these compounds could be converted by the Mb(H64V,V68A,H93S)[Co(ppIX)] variant

Scheme 1. Substrate Scope for Mb(H64V,V68A,H93S)[Co(ppIX)]-Catalyzed Cyclopropanation of Vinylarenes with EDA^a



^aReaction conditions: 10 mM olefin, 20 mM EDA, *E. coli* whole cells expressing Mb variants (OD₆₀₀ = 80) in 50 mM phosphate buffer (pH 7.2). ^bBased on GC conversion. ^cFor *trans*-(1*S*,2*S*) product. ^dUsing 5 mM olefin and 10 mM EDA. Enantiomeric excess not determined.

into the corresponding cyclopropanation products 7b–15b in moderate to good efficiency (30–88% product conversion). The results with 7b–9b indicate that substitutions at the ortho, meta, and para positions of the benzene ring are well tolerated by the Mb variant. Both electron-rich (11a) and -deficient (12a) styrene derivatives were efficiently converted (70–88% yield). More sterically hindered α,α-disubstituted and heterocycle-containing olefins also successfully participated in the reaction to afford the corresponding cyclopropanes 13b–15b in good yields (38–59%). Thus, despite a generally reduced catalytic activity compared to Mb-(H64V,V68A),^{2a,b} the Mb(H64V,V68A,H93S)[Co(ppIX)] variant features a comparably broad substrate scope across structurally different vinylarenes.

Across all the tested substrates, Mb(H64V,V68A,H93S)-[Co(ppIX)] was found to favor the formation of the *trans*-cyclopropanation product but with overall reduced diastereoselectivity (i.e., from 6:4 to 2:1 ratio for *trans*:*cis*) compared to Mb(H64V,V68A) (>98:2 dr).^{2a,b} As an exception, 7b was obtained with high diastereoselectivity (98:2 *trans*:*cis*). Similarly, Mb(H64V,V68A,H93S)[Co(ppIX)] maintains preference for the formation of the (1*S*,2*S*)-configured product but with significantly reduced enantioselectivity (e.g., 11–57% ee for 7b–11b) compared to Mb(H64V,V68A) (95–99% ee),^{2a,b} especially for the α,α-disubstituted olefins (3–4% ee for 13b–15b). Interestingly, parallel experiments with Mb-(H64V,V68A)[Co(ppIX)] showed that this metallo-substituted variant displays higher *trans*-(1*S*,2*S*)-selectivity in these reactions compared to Mb(H64V,V68A,H93S)[Co(ppIX)] (Scheme S1). Thus, the general reduction in stereoselectivity observed with Mb(H64V,V68A,H93S)[Co(ppIX)] vs Mb-(H64V,V68A) can be attributed to both the metal substitution and the mutation of the proximal ligand (His → Ser). This result is not entirely surprising given that (a) the active site mutations in Mb(H64V,V68A) were optimized for high *trans*-(1*S*,2*S*)-selectivity in the presence of the native histidine-ligated heme cofactor and (b) both the metal substitution and the structural change induced by the His93 → Ser substitution are likely to alter the orientation of the metalloporphyrin within the core of the protein, thereby affecting the asymmetric induction effect imposed by the protein scaffold during this reaction. Indeed, a significant shift in diastereoselectivity for styrene cyclopropanation with EDA was also noted upon substitution of the proximal cysteine with serine in a cytochrome P450 enzyme (22:78 vs 76:24 *cis*:*trans*, respectively).^{3b} Altogether, the results above showed that Mb(H64V,V68A,H93S)[Co(ppIX)] could be successfully applied to the cyclopropanation of a variety of aryl-substituted olefins, albeit reoptimization of its active site would be required for enhancing its stereoselectivity.

CONCLUSIONS

In summary, we have developed a novel biocatalytic strategy based on an engineered myoglobin-based carbene transferase for the chemoselective cyclopropanation of olefin substrates bearing unprotected Y–H groups (Y = N, Si). This transformation, unattainable using previously available carbene transfer (bio)catalysts, opens the way to the selective carbene-mediated functionalization of olefins in the presence of inherently more reactive Y–H groups. As emerged from the analysis of a systematic library of cofactor-modified Mb variants, the unique and atypical reactivity of Mb-(H64V,V68A,H93S)[Co(ppIX)] compared to Mb and other

hemoproteins is specifically induced by the combination of a non-native metal (Co) and non-native residue (Ser) at the proximal axial site of the metalloporphyrin cofactor. While featuring inverted chemoselectivity in carbene transfer reactions compared to the histidine-ligated Fe-containing counterpart (i.e., C=C > N–H > Si–H vs N–H > Si–H \gg C=C and S–H > N–H vs N–H > S–H), Mb-(H64V,V68A,H93S)[Co(ppIX)] features comparable stability, ease of expression in *E. coli*, and broad substrate scope in the cyclopropanation of vinylarenes with EDA. Further engineering of this scaffold (e.g., through active site mutagenesis)^{2a,b} is expected to improve its stereoselectivity, which is currently modest. The present studies highlight the functional plasticity of myoglobin as a carbene transferase and illustrate how modulation of the cofactor environment within this metalloprotein scaffold can provide a promising strategy for tuning its reactivity in the context of abiotic carbene transfer reactions. Further studies are warranted to elucidate the factors underlying the atypical reactivity of the Mb-(H64V,V68A,H93S)[Co(ppIX)] catalyst.

EXPERIMENTAL SECTION

General Information. All chemicals and reagents were purchased from commercial suppliers (Sigma-Aldrich, Alfa Aesar, TCI, Oakwood Chemicals, Combi Blocks) and used without any further purification unless otherwise stated. EDA was purchased from Sigma-Aldrich as 87% m/v solution in dichloromethane. Dimethyl(4-vinylphenyl)silane **3a** and 4-(dimethylsilyl)aniline **4a** were synthesized according to a previously reported procedure.⁶ Authentic racemic standards for the cyclopropanation products **7b–15b** and **20b** were synthesized and characterized as described previously.^{2a,b} All dry organic reactions were carried out under argon in oven-dried glassware with magnetic stirring using standard gastight syringes, cannulae, and septa. ¹H and ¹³C NMR spectra were measured on Bruker DPX-400 (operating at 400 MHz for ¹H and 100 MHz for ¹³C) or Bruker DPX-500 (operating at 500 MHz for ¹H and 125 MHz for ¹³C). Tetramethylsilane (TMS) served as the internal standard (0 ppm) for ¹H NMR, and the residual proton signal of the solvents was used as the internal standard for ¹³C NMR. HRMS analyses were performed using a Q Exactive Plus Mass Spectrometer at the Proteomics Facility of the University of Rochester. Silica gel chromatography purifications were carried out using AMD Silica Gel 60 230–400 mesh. Thin layer chromatography (TLC) was carried out using Merck Millipore TLC silica gel 60 F254 glass plates.

Growth Media. Enriched M9 media was prepared as follows. For 1 L, 770 mL of deionized H₂O was added with 200 mL of M9 salts (5 \times) solution, 20 mL of glucose (20% m/v), 10 mL of casamino acids (20% m/v), 1 mL of MgSO₄ (2 M), and 100 μ L of CaCl₂ (1 M). The M9 salt (5 \times) solution was prepared by dissolving 34 g of Na₂HPO₄, 15 g of K₂HPO₄, 2.5 g of NaCl, 5 g of NH₄Cl in 1 L of deionized H₂O and sterilized by autoclaving. The casamino acids and MgSO₄ solutions were autoclaved separately. The CaCl₂ and glucose stock solutions were sterilized by filtration. Enriched M9 agar plates were prepared by adding 17 g of agar to 1 L of enriched M9 media containing all of the aforementioned components at the specified concentrations with the exception of glucose and CaCl₂, which were added immediately prior to plating. To media and plates was added ampicillin to a final concentration of 100 mg/L and, then chloramphenicol was added to a final concentration of 34 mg/L.

Recombinant Expression of Myoglobins Containing Artificial Metalloporphyrins. All myoglobin variants were expressed from pET22-based vectors containing the target gene under a T7 promoter. The recombinant protein was engineered with a C-terminal polyhistidine tag. *E. coli* C41(DE3) cells expressing the heme transporter ChuA (T7 promoter) and GroES/EL chaperon proteins (araBAD promoter) were prepared via transformation with the plasmid pGroES/EL-ChuA.¹⁶ *E. coli* C41(DE3) cells containing the

pGroES/EL-ChuA plasmid were transformed with the pET22 vector encoding the desired Mb variant and selected on M9 agar plates containing ampicillin (100 mg/L) and chloramphenicol (34 mg/L). Single colonies were used to inoculate 5 mL of enriched M9 media supplemented with ampicillin and chloramphenicol followed by incubation at 37 °C with shaking (180 rpm) for 10–15 h. At an OD₆₀₀ of 0.8 to 1.0, the desired cofactor was added directly to the expression culture to a final concentration of ~30 mg/L followed by induction of protein expression with IPTG and arabinose at a final concentration of 1 mM. Cells were incubated at 20 °C with shaking (180 rpm) for 20–24 h. After harvesting, the cell pellets were resuspended in 20 mL of Ni NTA lysis buffer (50 mM KPi, 250 mM NaCl, 10 mM histidine, pH 8.0), lysed by sonication, and clarified by centrifugation (14,000 rpm, 4 °C, 30 min). When using *E. coli* in whole cell reactions, harvested cells were resuspended in 50 mM KPi pH 7.2 and stored at 4 °C for no longer than 12 h.

Protein Purification. Clarified lysate was transferred to a Ni-NTA column equilibrated with Ni-NTA lysis buffer. The resin was washed with 50 mL of Ni-NTA lysis buffer followed by 50 mL of Ni-NTA wash buffer (50 mM KPi, 250 mM NaCl, 20 mM Histidine, pH 8.0). Proteins were eluted with Ni-NTA elution buffer (50 mM KPi, 250 mM NaCl, 250 mM histidine, pH 7.0). After elution from the Ni-NTA column, the protein was buffer exchanged against 50 mM KPi buffer (pH 7.0) using 10 kDa Centricon filters. The concentrations of the Mb variants were calculated using the following extinction coefficients: $\epsilon_{410} = 157 \text{ mM}^{-1} \text{ cm}^{-1}$ for Fe(ppIX)-containing variants, $\epsilon_{470} = 60 \text{ mM}^{-1} \text{ cm}^{-1}$ for Mn(ppIX)-containing variants, $\epsilon_{424} = 152.5 \text{ mM}^{-1} \text{ cm}^{-1}$ for Co(ppIX)-containing variants, and $\epsilon_{405} = 122 \text{ mM}^{-1} \text{ cm}^{-1}$ for Rh(mpIX)-containing variants.

General Procedure for Biocatalytic Reactions with Whole Cells and Purified Protein. Under standard reaction conditions, 500 μ L scale reactions were carried out using 10–20 μ M Mb variant, 10 mM substrate, 10 mM EDA, and 10 mM sodium dithionite. TCEP (10 mM) was also added to the reactions with **6a** to prevent disulfide formation. In a typical procedure, a solution containing the desired myoglobin variant in potassium phosphate buffer (50 mM, pH 7.0) with sodium dithionite was prepared in an anaerobic chamber. Reactions were initiated by addition of 10 μ L of olefin followed by the addition of 10 μ L of EDA from 0.5 M stock solutions, and the reaction mixtures were stirred in the chamber for 12 h at room temperature. Whole-cell reactions were performed using *E. coli* C41(DE3) cells prepared using the method described above. Cell suspensions were transferred to an anaerobic chamber and diluted to the indicated cell density (OD₆₀₀: 40–80) with 50 mM KPi pH 7.2. Reactions were initiated by addition of 10 μ L of olefin followed by the addition of 10 μ L of EDA from 0.5 M stock solutions, and the mixtures were stirred in the chamber for 12 h at room temperature.

Product Analysis. The reactions with **1a**, **3a**, **4a**, and **5a** were analyzed by adding 20 μ L of internal standard (benzodioxole, 50 mM in ethanol) to the reaction mixture followed by extraction with 400 μ L of dichloromethane and analysis by gas chromatography (GC). GC analyses were carried out using a Shimadzu GC-2010 gas chromatograph equipped with an FID detector and a Chiral Cyclosil-B column (30 m \times 0.25 mm \times 0.25 μ m film). Separation method: 1 μ L injection, injector temp: 200 °C, detector temp: 300 °C. Gradient: column temperature set at 120 °C for 3 min, then to 150 °C at 0.8 °C/min, then to 245 °C at 25 °C/min. Total run time was 28.60 min. For the reactions with **6a**, the DCM extraction solution was evaporated, and the residue was redissolved in 300 μ L of methanol containing 10 mM TCEP, followed by HPLC analysis using a Shimadzu LC-2010A instrument equipped with a UV–vis detector. Analytical conditions: Thermo Fisher Scientific Hypersil GOLD C₁₈ column (250 \times 4.6 mm); UV detection: 254 nm; flow rate: 1.0 mL/min; solvent A: 1% trifluoroacetic acid in H₂O; solvent B: 1% trifluoroacetic acid in acetonitrile; gradient: 0–3 min: 30% B; 3–21 min: 30% B to 90% B; 21–24 min: 90% B; 24–24.5 min: 90% B to 30% B; 24.5–30 min: 30% B. Retention times: 3.82 min for 4-aminothiophenol; 4.89 min for S–H insertion product; 13.57 min for N–H insertion product; 14.91 min for double insertion product. Calibration curves for quantification of each single insertion product

were constructed using authentic standards prepared synthetically or enzymatically as described below. All measurements were performed at least in duplicate.

CD Analyses and T_m Determination. Circular dichroism (CD) spectroscopy and thermal denaturation analysis were performed using a JASCO J-1100 CD spectrophotometer equipped with variable temperature/wavelength denaturation software. Far UV CD spectra (250–190 nm) were obtained using 3 μ M solutions of purified Mb variant in 50 mM potassium phosphate buffer (pH 7.0) and recorded at 20 °C at a scan rate of 50 nm/min with a bandwidth of 1 nm and an averaging time of 10 s per measurement. Thermal denaturation curves were measured by monitoring the change in molar ellipticity at 222 nm (θ_{222}) over a temperature range from 20 to 100 °C. The temperature increase was set to 0.5 °C per minute with an equilibration time of 10 s. Data integration time for the melt curve was set to 4 s with a bandwidth of 1 nm. Linear baselines for the folded (θ_f) and unfolded state (θ_u) were generated. Melting temperature (T_m) was determined using the low temperature ($\theta_f = m_f T + b_f$) and high temperature ($\theta_u = m_u T + b_u$) equations fitted to the experimental data before and after global unfolding, respectively. These data were normalized and converted to fraction of folded protein (F_f) vs temperature plots, and the resulting curve was fitted to a sigmoidal equation (θ_{fit}) via nonlinear regression analysis in SigmaPlot from which apparent melting temperatures were derived.

Ethyl 2-(dimethyl(phenyl)silyl)acetate (1b). Ethyl 2-(dimethyl(phenyl)silyl)acetate **1b** was synthesized according to a modification of a reported procedure.⁶ Dimethyl(phenyl)silane **1a** (136 mg, 2.00 mmol, 1 equiv) and $\text{Rh}_2(\text{OAc})_4$ (4.4 mg, 10 μ mol, 1 mol %) were added to a flame-dried 10 mL round-bottom flask under an argon atmosphere, dissolved in anhydrous DCM (4 mL), and subsequently cooled to –78 °C. A solution of EDA (87%, 131 mg, 1.00 mmol, 1 equiv) in anhydrous DCM (1 mL) was added dropwise with a syringe pump over a period of 30 min. The reaction mixture was allowed to reach room temperature and stirred for 16 h. The solvent was removed under reduced pressure, and the crude product was purified via column chromatography on silica gel (0–7.5% EtOAc/pentanes) to yield ethyl 2-(dimethyl(phenyl)silyl)acetate **1b** as a clear oil (99.4 mg, 0.45 mmol, 45% yield). $R_f = 0.34$ (7.5% EtOAc/pentanes). $^1\text{H NMR}$ (CDCl_3 , 500 MHz): δ 7.51 (m, 2H), 7.34 (m, 3H), 3.98 (q, $J = 7.2$, 2H), 2.06 (s, 2H), 1.12 (t, $J = 7.0$ Hz, 3H), 0.36 (s, 6H). $^{13}\text{C NMR}$ (CDCl_3 , 125 MHz): δ 172.7, 137.7, 134.1, 130.0, 128.4, 60.4, 26.7, 14.7, –2.6. GC-MS m/z (% relative intensity): 207 (46.5), 177 (29.9), 165 (84.3), 145 (71.6), 135 (100.0)

Ethyl 2-(4-(Dimethylsilyl)phenyl)cyclopropanecarboxylate (3b). *E. coli* C41(DE3) cells expressing the variant Mb(H64V,V68A,H93S)-[Co(ppIX)] were prepared and harvested according to the protocol described above. In an anaerobic chamber (0 ppm of O_2 , 2.5% H_2 atmosphere), the whole cell suspension was diluted to an OD_{600} of 80 with argon purged phosphate buffer (50 mM, pH 7.2). A solution of dimethyl(4-vinylphenyl)silane **3a** (50.0 mg, 0.31 mmol, 1 equiv) in methanol (0.75 mL) was added dropwise while stirring to 28.5 mL of the whole cell suspension in an Erlenmeyer flask. The reaction was initiated by the dropwise addition of a solution of EDA (87%, 29.5 mg, 0.23 mmol, 0.75 equiv) in methanol (0.75 mL). The reaction mixture was stirred at room temperature for 16 h and extracted with DCM (3 \times 30 mL). The combined organic layers were dried over sodium sulfate and concentrated under reduced pressure. The crude product was purified by column chromatography on silica gel (0–7.5% Et₂O/pentanes), and the fractions were analyzed by gas chromatography with a chiral column to separate the cis (4.5 mg, 0.017 mmol, 1%) **3b-cis** and trans isomers (3.9 mg, 0.015 mmol, 1%) **3b-trans** and as clear oils. The configuration of **3b** was assigned by comparison to the splitting pattern in the $^1\text{H NMR}$ in alignment with the previously determined cis and trans isomers of **10b** (see Supporting Information). **3b-cis**: $R_f = 0.44$ (7.5% Et₂O/pentanes). $^1\text{H NMR}$ (CD_2Cl_2 , 500 MHz): δ 7.43 (d, $J = 8.0$ Hz, 2H), 7.08 (d, $J = 7.5$ Hz, 2H), 4.36 (m, 1H), 4.11 (q, $J = 7.2$ Hz, 2H), 4.45 (m, 1H), 1.87 (m, 1H), 1.54 (m, 1H), 1.29 (m, 1H), 1.23 (t, $J = 7.0$ Hz, 3H), 0.30 (d, $J = 4.0$ Hz, 6H). $^{13}\text{C NMR}$ (CD_2Cl_2 , 125 MHz): δ 171.2, 138.6, 135.8, 134.1, 129.4, 60.6, 25.9, 22.2, 14.4, 11.5, –3.6. GC-MS

m/z (% relative intensity): 248 (79.0), 233 (33.0), 201 (44.6), 144 (55.6), 129 (59.8), 115 (100.0). **3b-trans**: $R_f = 0.61$ (7.5% Et₂O/pentanes). $^1\text{H NMR}$ (CD_2Cl_2 , 500 MHz): δ 7.43 (d, $J = 8.0$ Hz, 2H), 7.08 (d, $J = 7.5$ Hz, 2H), 4.36 (m, 1H), 4.11 (q, $J = 7.2$ Hz, 2H), 4.45 (m, 1H), 1.87 (m, 1H), 1.54 (m, 1H), 1.29 (m, 1H), 1.23 (t, $J = 7.0$ Hz, 3H), 0.30 (d, $J = 4.0$ Hz, 6H). $^{13}\text{C NMR}$ (CD_2Cl_2 , 125 MHz): δ 173.5, 142.0, 135.8, 134.7, 126.2, 61.2, 26.5, 24.8, 17.4, 14.6, –3.5. GC-MS m/z (% relative intensity): 248 (83.3), 233 (33.5), 201 (43.7), 114 (56.6), 129 (62.7), 115 (100.0). HRMS (ESI) m/z : [M + H]⁺ calcd for C₁₄H₂₁O₂Si 249.1311; found 249.1303.

Ethyl 2-(Dimethyl(4-vinylphenyl)silyl)acetate (3c). Ethyl 2-(dimethyl(4-vinylphenyl)silyl)acetate **3c** was synthesized according to a modification of a previously reported procedure.⁶ Dimethyl(4-vinylphenyl)silane **3a** (150 mg, 0.92 mmol, 1 equiv) and $\text{Rh}_2(\text{OAc})_4$ (4.0 mg, 9 μ mol, 1 mol %) were added to a flame-dried 10 mL round-bottom flask under an argon atmosphere, dissolved in anhydrous DCM (4 mL), and subsequently cooled to –78 °C. A solution of EDA (106 mg, 0.9 mmol, 1 equiv) in anhydrous DCM (1 mL) was added dropwise with a syringe pump over a period of 30 min. The reaction mixture was allowed to reach room temperature and stirred for 16 h. The solvent was removed under reduced pressure, and the crude product was purified via column chromatography on silica gel (0–4% EtOAc/hexanes) to yield ethyl 2-(dimethyl(4-vinylphenyl)silyl)acetate **3c** as a clear oil (36.7 mg, 0.15 mmol, 15% yield). $R_f = 0.48$ (4% EtOAc/hexanes). $^1\text{H NMR}$ (CDCl_3 , 500 MHz): δ 7.50 (d, $J = 8.0$, 2H), 7.41 (d, $J = 8.0$, 2H), 6.72 (dd, $J = 11.0$, 17.5, 1H), 5.79 (d, $J = 17.5$, 1H), 5.28 (d, $J = 11.0$, 1H), 4.05 (q, $J = 7.2$, 2H), 2.11 (s, 2H), 2.27 (t, $J = 7.3$ Hz, 3H), 0.40 (s, 6H). $^{13}\text{C NMR}$ (CDCl_3 , 125 MHz): δ 172.7, 138.8, 136.8, 133.9, 129.0, 125.8, 114.7, 60.1, 26.4, 14.5, –2.6. GC-MS m/z (% relative intensity): 233 (76.6), 191 (87.2), 163 (44.2), 161 (100.0), 147 (39.7), 145 (42.7). HRMS (ESI) m/z : [M + H]⁺ calcd for C₁₄H₂₁O₂Si 249.1311; found 249.1306.

Ethyl 2-(4-Aminophenyl)cyclopropanecarboxylate (4b). Compound **4b** was prepared according to the procedure described in Scheme S2. Di-*tert*-butyl dicarbonate/Boc₂O (1.174 g, 5.38 mmol, 3.2 equiv) and *N,N*-diisopropylethylamine/DIPEA (651 mg, 5.04 mmol, 3 equiv) were added to a solution of dimethyl(4-vinylphenyl)silane **3a** (200 mg, 1.68 mmol, 1 equiv) in DCM (30 mL). The reaction mixture was stirred overnight at room temperature and then refluxed at 40 °C until completion, which was monitored by TLC. To remove excess Boc₂O, the solvent was evaporated, and the crude residue was taken up in 10 mL of a 1:1 mixture of THF:water before addition of glycine (246 mg, 4.30 mmol) and Na₂CO₃ (910 mg, 8.60 mmol). After stirring overnight, THF was removed in vacuo, and the aqueous layer extracted with DCM (3 \times 10 mL). The combined organic layers were washed with brine (10 mL), dried over sodium sulfate, filtered, and concentrated under reduced pressure. Flash column chromatography on silica gel (25% Et₂O/pentanes) furnished *tert*-butyl (4-vinylphenyl)carbamate **16** as white flaky solid (284 mg, 1.29 mmol, 77% yield). $R_f = 0.63$ (25% Et₂O/pentanes). $^1\text{H NMR}$ (CDCl_3 , 500 MHz): δ 7.30–7.19 (m, 4H), 6.59 (dd, $J = 11.0$, 17.5 Hz, 1H), 6.43 (br, 1H), 5.58 (d, $J = 17.5$ Hz, 1H), 5.09 (d, $J = 11.0$ Hz, 1H), 1.45 (s, 9H). GC-MS m/z (% relative intensity): 219 (19.4), 163 (100.0), 119 (76.9).

To a flame-dried 10 mL round-bottom flask equipped with a stir bar were added *tert*-butyl (4-vinylphenyl)carbamate **16** (100 mg, 0.46 mmol, 1 equiv), $\text{Rh}_2(\text{OAc})_4$ (4.0 mg, 9 μ mol, 2 mol %), and anhydrous DCM (2.5 mL) under argon. After that, a solution of EDA (87%, 119 mg, 0.9 mmol, 2 equiv) in anhydrous DCM (2.5 mL) was slowly added dropwise with a syringe pump over a period of 4 h. The resulting reaction mixture was stirred at room temperature for 12 h after which the solvent was removed under reduced pressure, and the crude product was purified via column chromatography on silica gel (0–20% Et₂O/pentanes) to afford ethyl 2-(4-((*tert*-butoxycarbonyl)amino)phenyl)cyclopropanecarboxylate **17** as a colorless oil (23 mg, 0.075 mmol, 16% yield). $R_f = 0.36$ (25% Et₂O/pentanes). $^1\text{H NMR}$ (CDCl_3 , 500 MHz): δ 7.26 (d, $J = 10.5$ Hz, 2H), 7.02 (d, $J = 10.5$ Hz, 2H), 6.48 (br, 1H), 4.16 (q, $J = 9.0$ Hz, 2H), 2.47 (m, 1H), 1.83 (m, 1H), 1.54 (m, 1H), 1.51 (s, 9H), 1.28 (t, $J = 9.0$ Hz, 3H), 1.26 (m, 1H). $^{13}\text{C NMR}$ (CDCl_3 , 125 MHz): δ 173.6, 152.9, 137.0, 134.8,

126.9, 118.8, 80.6, 60.8, 28.5, 25.9, 24.1, 17.0, 14.4. GC-MS m/z (% relative intensity): 305 (16.8), 249 (70.2), 205 (22.1), 176 (51.2), 158 (36.6), 132 (100.0).

A solution of 2-(4-((*tert*-butoxycarbonyl)amino)phenyl)-cyclopropanecarboxylate **17** (20 mg, 0.065 mmol, 1 equiv) in DCM (0.5 mL) was cooled to 0 °C. Trifluoroacetic acid (0.5 mL) was added dropwise, and the reaction mixture was stirred for 2 h before removing the solvent under reduced pressure. The crude product was taken up in 1.5 mL of DCM, transferred to an Eppendorf tube, and washed with NaHCO₃ (1 mL). The aqueous layer was extracted with DCM (2 × 1 mL), and the combined organic layers were dried over sodium sulfate and centrifuged; the supernatant was decanted, and the solvent was removed in vacuo to yield ethyl 2-(4-aminophenyl)-cyclopropanecarboxylate **4b** as a yellow solid (11.3 mg, 0.055 mmol, 85% yield). R_f = 0.43 (40% EtOAc/hexanes). ¹H NMR (CDCl₃, 500 MHz): δ 6.91 (d, J = 8.0 Hz, 2H), 6.61 (d, J = 8.5 Hz, 2H), 4.16 (q, J = 7.0, 2H), 3.60 (br, 2H), 2.43 (m, 1H), 1.79 (m, 1H), 1.52 (m, 1H), 1.27 (t, J = 7.0 Hz, 3H), 1.23 (m, 1H). ¹³C NMR (CDCl₃, 125 MHz): δ 173.9, 145.1, 130.0, 127.4, 115.3, 60.7, 26.0, 23.9, 16.7, 14.4. GC-MS m/z (% relative intensity): 205 (44.0), 176 (23.6), 160 (21.1), 132 (100.0).

Ethyl 2-((4-Vinylphenyl)amino)acetate (4c). *E. coli* C41(DE3) cells expressing the variant Mb(H64V,V68A,H93C) were prepared and harvested according to the protocol described above. In an anaerobic chamber (0 ppm of O₂, 2.5% H₂ atmosphere), the whole cell suspension was diluted to an OD₆₀₀ of 80 with argon-purged 50 mM phosphate buffer (pH 7.2). A solution of 4-vinylaniline **4a** (48.0 mg, 0.40 mmol, 1 equiv) in methanol (1.0 mL) was added dropwise while stirring to 38 mL of the whole cell suspension in an Erlenmeyer flask. The reaction was initiated by the dropwise addition of a solution of EDA (87%, 52.4 mg, 0.40 mmol, 1 equiv) in methanol (1.0 mL). The reaction mixture was stirred at room temperature for 16 h and extracted with DCM (3 × 40 mL). The combined organic layers were dried over sodium sulfate and concentrated under reduced pressure. The crude product was purified by column chromatography on silica gel (0–20% Et₂O/pentanes) to yield ethyl 2-((4-vinylphenyl)amino)acetate **4c** (20.0 mg, 0.10 mmol, 25%) as a white solid. R_f = 0.31 (20% Et₂O/pentanes). ¹H NMR (CDCl₃, 500 MHz): δ 7.23 (d, J = 8.0 Hz, 2H), 6.53 (d, J = 8.0 Hz, 2H), 5.51 (d, J = 17.5 Hz, 1H), 5.01 (d, J = 10.5 Hz, 1H), 4.32 (br, 1H), 4.21 (q, J = 6.7 Hz, 2H), 3.87 (d, J = 4.5 Hz, 2H), 1.27 (t, J = 7.0 Hz, 3H). ¹³C NMR (CDCl₃, 125 MHz): δ 171.1, 146.9, 136.7, 128.1, 127.5, 113.0, 111.0, 61.5, 45.9, 14.3. GC-MS m/z (% relative intensity): 205 (25.8), 132 (100.0).

Ethyl 2-((4-(Dimethylsilyl)phenyl)amino)acetate (5b). *E. coli* C41(DE3) cells expressing the variant Mb(H64V,V68A) were prepared and harvested according to the protocol described above. Under an argon atmosphere, the cells were resuspended in argon purged 50 mM phosphate buffer (pH 7.2) and diluted to an OD₆₀₀ of 40. A solution of 4-(dimethylsilyl)aniline **5a** (60.5 mg, 0.40 mmol, 1 equiv) in ethanol (1.0 mL) was added dropwise while stirring to 38 mL of the whole cell suspension in an Erlenmeyer flask. A solution of EDA (87%, 52.6 mg, 0.40 mmol, 1 equiv) in ethanol (1.0 mL) was added dropwise over 4 h. The reaction mixture was stirred at room temperature for 16 h and extracted with DCM (3 × 40 mL). The combined organic layers were dried over sodium sulfate and concentrated under reduced pressure. The crude product was purified by column chromatography on silica gel (0–20% EtOAc/hexanes) to yield ethyl 2-(4-(dimethylsilyl)-phenyl)cyclopropanecarboxylate **5b** (40.0 mg, 0.17 mmol, 42%) as a clear oil. R_f = 0.48 (20% EtOAc/hexanes). ¹H NMR (CDCl₃, 500 MHz): δ 7.37 (d, J = 8.5 Hz, 2H), 6.62 (d, J = 8.5 Hz, 2H), 4.39 (m, 1H), 4.26 (q, J = 7.0 Hz, 2H), 3.91 (s, 2H), 1.31 (t, J = 7.3 Hz, 3H), 0.30 (d, J = 3.5 Hz, 6H). ¹³C NMR (CDCl₃, 125 MHz): δ 171.1, 148.0, 135.4, 124.8, 122.8, 61.5, 45.7, 14.3, –3.3. GC-MS m/z (% relative intensity): 237 (32.5), 164 (100.0). HRMS (ESI) m/z : [M + H]⁺ calcd for C₁₂H₂₀NO₂Si 238.1263; found 238.1260.

Ethyl 2-((4-Aminophenyl)dimethylsilyl)acetate (5c). Compound **5c** was prepared according to the procedure described in Scheme S3, which was adapted from a previously reported procedure.⁶ A solution of 4-(dimethylsilyl)aniline **5a** (50 mg, 0.33 mmol, 1 equiv) and

pyridine (52 mg, 0.66 mmol, 2 equiv) in anhydrous DCM (1 mL) was stirred for 10 min followed by the addition of benzyl chloroformate (68 mg, 0.40 mmol, 1.2 equiv). The reaction mixture was stirred overnight after which the solvent was removed under reduced pressure. Benzyl (4-(dimethylsilyl)phenyl)carbamate **18** was obtained as a white flaky solid (62 mg, 0.22 mmol, 66% yield) after purification by column chromatography on silica gel (5% EtOAc/hexanes). R_f = 0.38 (5% EtOAc/hexanes). ¹H NMR (CDCl₃, 500 MHz): δ 7.49–7.35 (m, 9H), 6.71 (br, 1H), 5.21 (s, 2H), 4.41 (quin, J = 3.5 Hz, 1H), 0.33 (d, J = 3.5 Hz, 6H). ¹³C NMR (CDCl₃, 125 MHz): δ 153.3, 138.9, 136.1, 135.1, 132.0, 128.8, 128.5, 128.5, 118.2, 67.2, –3.5. GC-MS m/z (% relative intensity): 285 (82.5), 241 (25.9), 226 (34.0), 162 (51.7), 150 (100.0).

Benzyl (4-(dimethylsilyl)phenyl)carbamate **18** (50 mg, 0.18 mmol, 1 equiv) and Rh₂(OAc)₄ (1 mg, 2 μmol, 1 mol %) were added to a flame-dried 5 mL round-bottom flask under an argon atmosphere, dissolved in anhydrous DCM (1 mL), and subsequently cooled to –78 °C. A solution of EDA (23.6 mg, 0.18 mmol, 1 equiv) in anhydrous DCM (1 mL) was added dropwise with a syringe pump over a period of 30 min. The reaction mixture was allowed to reach room temperature and stirred for 16 h. The solvent was removed under reduced pressure, and the crude product was purified via column chromatography on silica gel (0–20% EtOAc/hexanes) to afford ethyl 2-((4-((benzyloxy)carbonyl)amino)phenyl)-dimethylsilyl)acetate **19** as a clear oil (6.0 mg, 0.018 mmol, 9% yield). R_f = 0.49 (20% EtOAc/hexanes). ¹H NMR (CDCl₃, 400 MHz): δ 7.48–7.34 (m, 9H), 6.70 (br, 1H), 5.20 (s, 2H), 4.03 (q, J = 7.1 Hz, 2H), 2.08 (s, 2H), 1.16 (t, J = 7.1 Hz, 3H), 0.38 (s, 6H). ¹³C NMR (CDCl₃, 125 MHz): δ 172.8, 153.2, 130.1, 136.1, 134.7, 131.5, 128.8, 128.6, 128.5, 118.1, 67.3, 60.1, 26.5, 14.5, –2.6. APCI-MS (TLC) m/z : 372, 284.

A flame-dried 5 mL round-bottom flask was charged with ethyl 2-((4-((benzyloxy)carbonyl)amino)phenyl)dimethylsilyl)acetate **19** (10 mg, 0.027 mmol, 1 equiv), 10% Pd/C (4 mg), and anhydrous EtOH (1 mL) under an argon atmosphere. The reaction mixture was purged with H₂ for 30 min and stirred overnight under a H₂ atmosphere. After exchanging the atmosphere with argon, the residue was diluted with EtOAc, filtered over Celite, concentrated under reduced pressure, and purified by column chromatography on silica gel (10–50% EtOAc/hexanes) to give ethyl 2-((4-aminophenyl)-dimethylsilyl)acetate **5c** as a yellow oil (4.1 mg, 0.017 mmol, 64%). R_f = 0.55 (50% EtOAc/hexanes). ¹H NMR (CDCl₃, 500 MHz): δ 6.96 (d, J = 5.0, 2H), 6.59 (d, J = 5.0 Hz, 2H), 4.24 (q, J = 5.0 Hz, 2H), 2.67 (s, 2H), 1.95 (t, J = 5.0 Hz, 3H), 1.31 (s, 6H). ¹³C NMR spectrum could not be collected due to the instability of product **5c** in the NMR solvent. GC-MS m/z (% relative intensity): 237 (20.6), 222 (27.4), 180 (69.1), 150 (100.0), 136 (31.8). HRMS (ESI) m/z : [M + H]⁺ calcd for C₁₂H₂₀NO₂Si 238.1263; found 238.1256.

Ethyl 2-((4-Mercaptophenyl)amino)acetate (6b). This compound was synthesized according to a modification of a previously reported procedure (Scheme S4).²⁰ 4-Aminothiophenol **6a** (200 mg, 1.60 mmol, 1 equiv) was dissolved in a minimal amount of MeOH (2 mL) and DMSO (60 μL) and treated with I₂ (162 mg, 0.64 mmol, 0.4 equiv). After consumption of the starting material (3 h), the solvent was removed under reduced pressure, and the crude product was purified by column chromatography on silica gel (20–80% EtOAc/hexanes) to yield 4,4'-disulfaneyldianiline (**20**) as a yellow solid (104 mg, 0.42 mmol, 52% yield). R_f = 0.26 (50% EtOAc/hexanes). ¹H NMR (CDCl₃, 500 MHz): δ 7.22 (d, J = 7.0 Hz, 2H), 6.55 (d, J = 8.5 Hz, 2H), 3.75 (br, 4H). ¹³C NMR (CDCl₃, 125 MHz): δ 147.7, 134.4, 124.7, 115.5. GC-MS m/z (% relative intensity): 248 (38.5), 124 (78.9), 125 (100.0).

To a flame-dried 10 mL round-bottom flask equipped with a stir bar were added 4,4'-disulfaneyldianiline **20** (48 mg, 0.19 mmol, 1 equiv), Rh₂(OAc)₄ (2 mg, 4 μmol, 2 mol %), and anhydrous DCM (1 mL) under argon. After that, a solution of EDA (43 mg, 0.38 mmol, 2 equiv) in anhydrous DCM (1 mL) was slowly added dropwise over a period of 30 min. The resulting reaction mixture was stirred at room temperature for 16 h. The solvent was removed under reduced pressure, and the crude product was purified via column

chromatography on silica gel (20–80% EtOAc/hexanes) to afford ethyl 2-((4-mercaptophenyl)amino)acetate (**6b**) as a yellow solid (20 mg, 0.089 mmol, 47% yield). R_f = 0.31 (50% EtOAc/hexanes). ^1H NMR (CDCl_3 , 500 MHz): δ 7.25 (d, J = 7.5 Hz, 2H), 6.47 (d, J = 7.0 Hz, 2H), 4.41 (br, 1H), 4.22 (q, J = 6.5 Hz, 2H), 4.09 (br, 1H), 3.85 (s, 2H), 1.27 (t, J = 6.3 Hz, 3H). ^{13}C NMR (CDCl_3 , 125 MHz): δ 170.8, 147.5, 134.2, 125.4, 113.3, 61.6, 45.2, 14.3. GC-MS m/z (% relative intensity): 211 (36.0), 128 (100.0), 136 (23.8), 109 (11.3).

Ethyl 2-((4-aminophenyl)thio)acetate (6c). This compound was synthesized according to a modification of a previously reported procedure (Scheme S5).²¹ A flame-dried 25 mL 2-neck round-bottom flask was charged with 4-aminothiophenol **6a** (200 mg, 1.60 mmol, 1 equiv) and anhydrous THF (10 mL) under argon. The solution was cooled to -30°C , and sodium hydride (66 mg, 1.66 mmol, 1.04 equiv) was added in portions. After the reaction mixture was allowed to reach 0°C , it was cooled again to -30°C for the addition of ethyl bromoacetate (264 mg, 1.58 mmol, 0.99 equiv) and stirred overnight at room temperature. The solvent was removed under reduced pressure, and the crude product was taken up in EtOAc (20 mL) and water (20 mL). The aqueous layer was extracted with EtOAc (3×20 mL). The combined organic layers were washed with aq. saturated NaHCO_3 (10 mL), brine (10 mL), and water (10 mL), dried over Na_2SO_4 , and concentrated under reduced pressure. Purification by column chromatography on silica gel (0–40% EtOAc/hexanes) afforded ethyl 2-((4-aminophenyl)thio)acetate (**6c**) as a yellow oil (268 mg, 1.26 mmol, 79% yield). R_f = 0.54 (20% EtOAc/hexanes). ^1H NMR (CDCl_3 , 500 MHz): δ 7.29 (d, J = 6.5 Hz, 2H), 6.60 (d, J = 7.0 Hz, 2H), 4.13 (t, J = 6.7 Hz, 2H), 3.76 (br, 2H), 3.45 (s, 2H), 1.21 (t, J = 6.5 Hz, 3H). ^{13}C NMR (CDCl_3 , 125 MHz): δ 170.3, 147.0, 135.0, 121.8, 115.6, 61.4, 39.3, 14.2. GC-MS m/z (% relative intensity): 211 (84.2), 212.1 (10.9), 138 (25.8), 124 (100.0).

■ ASSOCIATED CONTENT

Supporting Information

The Supporting Information is available free of charge on the ACS Publications website at DOI: 10.1021/acs.joc.8b00946.

Additional experimental data, synthetic schemes, and NMR spectra for all new compounds (PDF)

■ AUTHOR INFORMATION

Corresponding Author

*E-mail: rfasan@ur.rochester.edu.

ORCID

Viktoria Steck: 0000-0003-0833-3531

Rudi Fasan: 0000-0003-4636-9578

Author Contributions

[†]E.J.M. and V.S. contributed equally to this work.

Notes

The authors declare no competing financial interest.

■ ACKNOWLEDGMENTS

This work was supported in part by the U.S. National Science Foundation (NSF) grant CHE-1609550 and in part by the U.S. National Institute of Health (NIH) grant GM098628. E.J.M. acknowledges support from the NIH Graduate Training Grant T32GM118283. MS instrumentation was supported by the U.S. NSF grant CHE-0946653. The authors are grateful to Dr. Jermaine Jenkins and the Structure Biology & Biophysics Facility at the University of Rochester for providing access to the CD instrumentation.

■ REFERENCES

(1) (a) Miller, D. J.; Moody, C. J. Synthetic Applications of the O-H Insertion Reactions of Carbenes and Carbenoids Derived from

Diazocarbonyl and Related Diazo-Compounds. *Tetrahedron* **1995**, *51*, 10811–10843. (b) Doyle, M. P.; Forbes, D. C. Recent Advances in Asymmetric Catalytic Metal Carbene Transformations. *Chem. Rev.* **1998**, *98*, 911–936. (c) Lebel, H.; Marcoux, J. F.; Molinaro, C.; Charette, A. B. Stereoselective Cyclopropanation Reactions. *Chem. Rev.* **2003**, *103*, 977–1050. (d) Zhang, Z. H.; Wang, J. B. Recent Studies on the Reactions of Alpha-Diazocarbonyl Compounds. *Tetrahedron* **2008**, *64*, 6577–6605. (e) Davies, H. M. L.; Morton, D. Guiding Principles for Site Selective and Stereoselective Intermolecular C-H Functionalization by Donor/Acceptor Rhodium Carbenes. *Chem. Soc. Rev.* **2011**, *40*, 1857–1869. (f) Zhu, S. F.; Zhou, Q. L. Transition-Metal-Catalyzed Enantioselective Heteroatom-Hydrogen Bond Insertion Reactions. *Acc. Chem. Res.* **2012**, *45*, 1365–1377.

(2) (a) Bordeauxaux, M.; Tyagi, V.; Fasan, R. Highly Diastereoselective and Enantioselective Olefin Cyclopropanation Using Engineered Myoglobin-Based Catalysts. *Angew. Chem., Int. Ed.* **2015**, *54*, 1744–1748. (b) Bajaj, P.; Sreenilayam, G.; Tyagi, V.; Fasan, R. Gram-Scale Synthesis of Chiral Cyclopropane-Containing Drugs and Drug Precursors with Engineered Myoglobin Catalysts Featuring Complementary Stereoselectivity. *Angew. Chem., Int. Ed.* **2016**, *55*, 16110–16114. (c) Sreenilayam, G.; Moore, E. J.; Steck, V.; Fasan, R. Metal Substitution Modulates the Reactivity and Extends the Reaction Scope of Myoglobin Carbene Transfer Catalysts. *Adv. Synth. Catal.* **2017**, *359*, 2076–2089. (d) Tinoco, A.; Steck, V.; Tyagi, V.; Fasan, R. Highly Diastereo- and Enantioselective Synthesis of Trifluoromethyl-Substituted Cyclopropanes Via Myoglobin-Catalyzed Transfer of Trifluoromethylcarbene. *J. Am. Chem. Soc.* **2017**, *139*, 5293–5296.

(3) (a) Coelho, P. S.; Brustad, E. M.; Kannan, A.; Arnold, F. H. Olefin Cyclopropanation Via Carbene Transfer Catalyzed by Engineered Cytochrome P450 Enzymes. *Science* **2013**, *339*, 307–310. (b) Coelho, P. S.; Wang, Z. J.; Ener, M. E.; Baril, S. A.; Kannan, A.; Arnold, F. H.; Brustad, E. M. A Serine-Substituted P450 Catalyzes Highly Efficient Carbene Transfer to Olefins in Vivo. *Nat. Chem. Biol.* **2013**, *9*, 485–487. (c) Gober, J. G.; Rydeen, A. E.; Gibson-O'Grady, E. J.; Leuthaeuser, J. B.; Fetrow, J. S.; Brustad, E. M. Mutating a Highly Conserved Residue in Diverse Cytochrome P450s Facilitates Diastereoselective Olefin Cyclopropanation. *ChemBioChem* **2016**, *17*, 394–397. (d) Gober, J. G.; Ghodge, S. V.; Bogart, J. W.; Wever, W. J.; Watkins, R. R.; Brustad, E. M.; Bowers, A. A. P450-Mediated Non-Natural Cyclopropanation of Dehydroalanine-Containing Thiopeptides. *ACS Chem. Biol.* **2017**, *2*, 1726–1731.

(4) (a) Wang, Z. J.; Peck, N. E.; Renata, H.; Arnold, F. H. Cytochrome P450-Catalyzed Insertion of Carbenoids into N-H Bonds. *Chem. Sci.* **2014**, *5*, 598–601. (b) Sreenilayam, G.; Fasan, R. Myoglobin-Catalyzed Intermolecular Carbene N-H Insertion with Arylamine Substrates. *Chem. Commun.* **2015**, *51*, 1532–1534.

(5) Tyagi, V.; Bonn, R. B.; Fasan, R. Intermolecular Carbene S-H Insertion Catalysed by Engineered Myoglobin-Based Catalysts. *Chem. Sci.* **2015**, *6*, 2488–2494.

(6) Kan, S. B. J.; Lewis, R. D.; Chen, K.; Arnold, F. H. Directed Evolution of Cytochrome C for Carbon-Silicon Bond Formation: Bringing Silicon to Life. *Science* **2016**, *354*, 1048–1051.

(7) (a) Sreenilayam, G.; Moore, E. J.; Steck, V.; Fasan, R. Stereoselective Olefin Cyclopropanation under Aerobic Conditions with an Artificial Enzyme Incorporating an Iron-Chlorin E6 Cofactor. *ACS Catal.* **2017**, *7*, 7629–7633. (b) Key, H. M.; Dydio, P.; Clark, D. S.; Hartwig, J. F. Abiological Catalysis by Artificial Haem Proteins Containing Noble Metals in Place of Iron. *Nature* **2016**, *534*, 534–537. (c) Reynolds, E. W.; McHenry, M. W.; Cannac, F.; Gober, J. G.; Snow, C. D.; Brustad, E. M. An Evolved Orthogonal Enzyme/Cofactor Pair. *J. Am. Chem. Soc.* **2016**, *138*, 12451–12458. (d) Reynolds, E. W.; Schwochert, T. D.; McHenry, M. W.; Watters, J. W.; Brustad, E. M. Orthogonal Expression of an Artificial Metalloenzyme for Abiotic Catalysis. *ChemBioChem* **2017**, *18*, 2380–2384. (e) Wolf, M. W.; Vargas, D. A.; Lehnert, N. Engineering of Rumb: Toward a Green Catalyst for Carbene Insertion Reactions. *Inorg. Chem.* **2017**, *56*, 5623–5635. (f) Oohora, K.; Meichin, H.; Zhao, L. M.; Wolf, M. W.; Nakayama, A.; Hasegawa, J.; Lehnert, N.;

Hayashi, T. Catalytic Cyclopropanation by Myoglobin Reconstituted with Iron Porphycene: Acceleration of Catalysis Due to Rapid Formation of the Carbene Species. *J. Am. Chem. Soc.* **2017**, *139*, 17265–17268.

(8) (a) Srivastava, P.; Yang, H.; Ellis-Guardiola, K.; Lewis, J. C. Engineering a Dirhodium Artificial Metalloenzyme for Selective Olefin Cyclopropanation. *Nat. Commun.* **2015**, *6*, 7789. (b) Rioz-Martinez, A.; Oelerich, J.; Segaud, N.; Roelfes, G. DNA-Accelerated Catalysis of Carbene-Transfer Reactions by a DNA/Cationic Iron Porphyrin Hybrid. *Angew. Chem., Int. Ed.* **2016**, *55*, 14136–14140.

(9) Talele, T. T. The "Cyclopropyl Fragment" Is a Versatile Player That Frequently Appears in Preclinical/Clinical Drug Molecules. *J. Med. Chem.* **2016**, *59*, 8712–8756.

(10) (a) Galardon, E.; Le Maux, P.; Simonneaux, G. Cyclopropanation of Alkenes, N-H and S-H Insertion of Ethyl Diazoacetate Catalysed by Ruthenium Porphyrin Complexes. *Tetrahedron* **2000**, *56*, 615–621. (b) Aviv, I.; Gross, Z. Iron Corroles and Porphyrins as Very Efficient and Highly Selective Catalysts for the Reactions of Alpha-Diazo Esters with Amines. *Synlett* **2006**, *2006*, 951–953. (c) Baumann, L. K.; Mbuvi, H. M.; Du, G.; Woo, L. K. Iron Porphyrin Catalyzed N-H Insertion Reactions with Ethyl Diazoacetate. *Organometallics* **2007**, *26*, 3995–4002. (d) Noels, A. F.; Demonceau, A.; Petiniot, N.; Hubert, A. J.; Teyssie, P. Transition-Metal-Catalyzed Reactions of Diazo-Compounds, Efficient Synthesis of Functionalized Ethers by Carbene Insertion into the Hydroxylic Bond of Alcohols. *Tetrahedron* **1982**, *38*, 2733–2739. (e) Zhu, S. F.; Cai, Y.; Mao, H. X.; Xie, J. H.; Zhou, Q. L. Enantioselective Iron-Catalysed O-H Bond Insertions. *Nat. Chem.* **2010**, *2*, 546–551.

(11) (a) Bagheri, V.; Doyle, M. P.; Taunton, J.; Claxton, E. E. A New and General-Synthesis of Alpha-Silyl Carbonyl-Compounds by Si-H Insertion from Transition-Metal Catalyzed-Reactions of Diazo Esters and Diazo Ketones. *J. Org. Chem.* **1988**, *53*, 6158–6160. (b) Andrey, O.; Landais, Y.; Planchenault, D. A One-Pot Synthesis of Alpha-(Alkoxysilyl)Acetic Esters. *Tetrahedron Lett.* **1993**, *34*, 2927–2930. (c) Wang, J. C.; Xu, Z. J.; Guo, Z.; Deng, Q. H.; Zhou, C. Y.; Wan, X. L.; Che, C. M. Highly Enantioselective Intermolecular Carbene Insertion to C-H and Si-H Bonds Catalyzed by a Chiral Iridium(III) Complex of a D-4-Symmetric Halterman Porphyrin Ligand. *Chem. Commun.* **2012**, *48*, 4299–4301. (d) Keipour, H.; Ollevier, T. Iron-Catalyzed Carbene Insertion Reactions of Alpha-Diazoesters into Si-H Bonds. *Org. Lett.* **2017**, *19*, 5736–5739.

(12) (a) Sambasivan, R.; Ball, Z. T. Metallopeptides for Asymmetric Dirhodium Catalysis. *J. Am. Chem. Soc.* **2010**, *132*, 9289–9291. (b) Yang, H.; Srivastava, P.; Zhang, C.; Lewis, J. C. A General Method for Artificial Metalloenzyme Formation through Strain-Promoted Azide-Alkyne Cycloaddition. *ChemBioChem* **2014**, *15*, 223–227.

(13) Zhang, K. D.; El Damaty, S.; Fasan, R. P450 Fingerprinting Method for Rapid Discovery of Terpene Hydroxylating P450 Catalysts with Diversified Regioselectivity. *J. Am. Chem. Soc.* **2011**, *133*, 3242–3245.

(14) Wei, Y.; Tinoco, A.; Steck, V.; Fasan, R.; Zhang, Y. Cyclopropanations Via Heme Carbenes: Basic Mechanism and Effects of Carbene Substituent, Protein Axial Ligand, and Porphyrin Substitution. *J. Am. Chem. Soc.* **2018**, *140*, 1649–1662.

(15) Vojtechovsky, J.; Chu, K.; Berendzen, J.; Sweet, R. M.; Schlichting, I. Crystal Structures of Myoglobin-Ligand Complexes at near-Atomic Resolution. *Biophys. J.* **1999**, *77*, 2153–2174.

(16) Bordeaux, M.; Singh, R.; Fasan, R. Intramolecular C(Sp³)H Amination of Arylsulfonyl Azides with Engineered and Artificial Myoglobin-Based Catalysts. *Bioorg. Med. Chem.* **2014**, *22*, 5697–5704.

(17) Kunze, C.; Bommer, M.; Hagen, W. R.; Uksa, M.; Dobbek, H.; Schubert, T.; Diekert, G. Cobamide-Mediated Enzymatic Reductive Dehalogenation Via Long-Range Electron Transfer. *Nat. Commun.* **2017**, *8*, 15858.

(18) Moore, E. J.; Zorine, D.; Hansen, W. A.; Khare, S. D.; Fasan, R. Enzyme Stabilization Via Computationally Guided Protein Stapling. *Proc. Natl. Acad. Sci. U. S. A.* **2017**, *114*, 12472–12477.

(19) Aller, E.; Brown, D. S.; Cox, G. G.; Miller, D. J.; Moody, C. J. Diastereoselectivity in the O-H Insertion Reactions of Rhodium Carbenoids Derived from Phenyl diazoacetates of Chiral Alcohols - Preparation of Alpha-Hydroxy and Alpha-Alkoxy Esters. *J. Org. Chem.* **1995**, *60*, 4449–4460.

(20) Bettanin, L.; Saba, S.; Galetto, F. Z.; Mike, G. A.; Rafique, J.; Braga, A. L. Solvent- and Metal-Free Selective Oxidation of Thiols to Disulfides Using I-2/DMSO Catalytic System. *Tetrahedron Lett.* **2017**, *58*, 4713–4716.

(21) Chen, B. B.; Chen, H. Y.; Gesicki, G. J. In Pat. Appl. EP0891325-B1; GD Searle LLC, 1996.